BIOCHEMISTRY
including biophysical chemistry & molecular biology

Article

pubs.acs.org/biochemistry

Kinetics and Intermediates of the Reaction of Fully Reduced *Escherichia coli* bo_3 Ubiquinol Oxidase with O_2

Istvan Szundi,[‡] Clive Kittredge,[‡,⊥] Sylvia K. Choi,[§] William McDonald,[‡] Jayashree Ray,[‡,#] Robert B. Gennis,[§] and Ólöf Einarsdóttir*[,‡]

[‡]Department of Chemistry and Biochemistry, University of California, Santa Cruz, California 95064, United States

[§]Department of Biochemistry and the Center for Biophysics and Computational Biology, University of Illinois, Urbana-Champaign, Illinois 61801, United States

ABSTRACT: Cytochrome bo_3 ubiquinol oxidase from *Escherichia coli* catalyzes the reduction of O_2 to water by ubiquinol. The reaction mechanism and the role of ubiquinol continue to be a subject of discussion. In this study, we report a detailed kinetic scheme of the reaction of cytochrome bo_3 with O_2 with steps specific to ubiquinol. The reaction was investigated using the CO flow-flash method, and time-resolved optical absorption difference spectra were collected from 1 μs to 20 ms after photolysis. Singular value decomposition-based global exponential fitting resolved five apparent lifetimes, 22 μs, 30 μs, 42 μs, 470 μs, and 2.0 ms. The reaction mechanism was derived by an algebraic kinetic analysis method using frequency-shifted spectra of known bovine states to identify the bo_3 intermediates. It shows 42 μs O_2 binding (3.8×10^7 M^{-1} s^{-1}), producing compound **A**, followed by faster (22 μs) heme *b* oxidation, yielding a mixture of $\mathbf{P_R}$ and **F**, and rapid heme *b* rereduction by ubiquinol (30 μs), producing the **F** intermediate and semiquinone. In the 470 μs step, the o_3 **F** state is converted into the o_3^{3+} oxidized state, presumably by semiquinone/ubiquinol, without the concomitant oxidation of heme *b*. The final 2 ms step shows heme *b* reoxidation and the partial rereduction of the binuclear center and, following O_2 binding, the formation of a mixture of **P** and **F** during a second turnover cycle. The results show that ubiquinol/semiquinone plays a complex role in the mechanism of O_2 reduction by bo_3, displaying kinetic steps that have no analogy in the Cu_A-containing heme-copper oxidases.

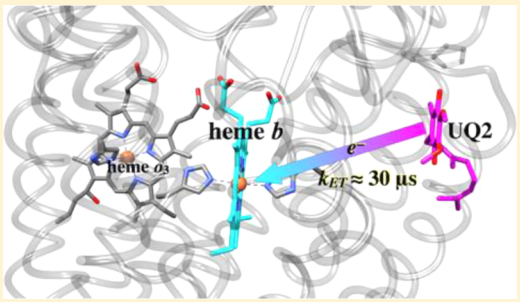

Cytochrome bo_3 from *Escherichia coli* belongs to the A-type superfamily of the heme-copper oxidases and is expressed under aerobic conditions.[1,2] The enzyme catalyzes the reduction of dioxygen to water by oxidizing ubiquinol (QH_2) to ubiquinone (Q) and couples the redox reaction to the translocation of protons across the plasma membrane.[3] The enzyme is also able to reduce nitric oxide (NO) to nitrous oxide (N_2O), although with low turnover.[4] The bo_3 enzyme contains four subunits, with the three redox centers, the low-spin heme *b*, and the binuclear center, heme *o* (o_3) and Cu_B, in subunit I;[5] the heme o_3/Cu_B site is analogous to the heme a_3/Cu_B site found in the mitochondrial cytochrome *c* oxidase, CcO.[6] The high-spin heme o_3 has the same structure as that of heme *a* except the formyl group is replaced by a methyl group.[7] Unlike the aa_3 oxidases, the bo_3 enzyme does not contain the dinuclear Cu_A center. Rather, heme *b* receives electrons from a bound ubiquinol molecule.[8] There is considerable experimental evidence indicating that cytochrome bo_3 has two ubiquinone binding sites, a low affinity site (Q_L), at which the substrate is oxidized from ubiquinol to ubiquinone, and a high affinity site, Q_H, which is proposed to mediate electron transfer from Q_L to the metals centers.[9−11] Figure 1 shows the active site of the *E. coli* bo_3 with ubiquinone-2 modeled into the proposed Q_H site.[5]

The kinetics of O_2 reduction to water has been extensively studied in the mitochondrial bovine heart enzyme using transient absorption spectroscopy in combination with the CO flow-flash method (see refs 12−14 for review), in which the reaction is initiated by photolyzing the CO-bound enzyme in the presence of O_2.[15] Four processes have been resolved, and the reaction has generally been analyzed in terms of a unidirectional sequential mechanism. In this mechanism, the fully reduced enzyme (**R**) binds O_2 to form compound **A**, followed by the simultaneous breaking of the O−O bond and the oxidation of the low-spin heme *a*, which generates the $\mathbf{P_R}$ intermediate. Subsequent proton uptake forms the oxyferryl (**F**) intermediate, concomitant with a partial rereduction of the low-spin heme *a* by Cu_A. This step is followed by proton uptake and electron transfer to the binuclear center to form the oxidized (**O**) intermediate (for review see refs 12−14).

Because of the complexity of the bovine enzyme and the general inability to assess the role of specific residues in ligand binding and electron and proton transfer through mutagenesis in this enzyme, bacterial heme-copper oxidases, including *E. coli* bo_3, are frequently used as models for the mitochondrial enzyme. Early transient absorption flow-flash studies on the reaction of O_2 with cytochrome bo_3 showed either monophasic

Received: May 13, 2014
Revised: July 23, 2014
Published: July 30, 2014

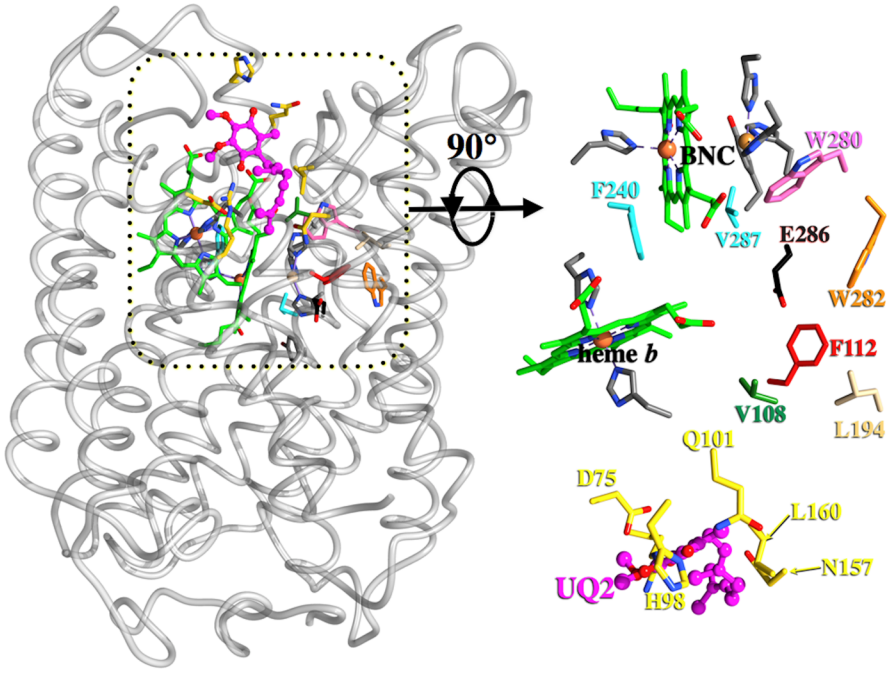

Figure 1. *E. coli* bo_3 subunit I (PDB 1FFT, 5) as viewed from within the bacterial membrane (left), and the binuclear center (BNC), low-spin heme *b*, and surrounding residues as viewed from the positive side of the bacterial membrane (right). Also included is a model of ubiquinol-2 in the proposed binding site of Abramson et al.[5]

or multiphasic kinetics depending on the isolation procedure.[8,16−18] Monophasic kinetics were observed when the enzyme was isolated using the detergent Triton (TX), which removed the bound ubiquinone, while multiphasic kinetics were observed for the ubiquinone-bound enzyme isolated with dodecylmaltoside (DM).[8] The mechanism of O_2 reduction by the ubiquinone-bound bo_3 has been postulated to be analogous to the unidirectional sequential mechanism discussed above for the bovine heart enzyme. Three kinetic phases, with time constants of 45 μs, 700 μs, and 4 ms, have been reported.[18] The first phase was assigned to the oxidation of heme o_3 and *b* and the formation of the "peroxy" (**P**) intermediate, while the second and third phases were attributed to electron transfer from ubiquinol (QH_2) to heme *b*, and electron transfer from heme *b* to the binuclear center, respectively.[18] The spectrum of the dioxygen-bound intermediate, compound **A**, was not resolved,[18] presumably because the O_2 binding is rate-limiting for the subsequent electron transfer process.

In this study, the reactions of O_2 and NO with the fully reduced *E. coli* bo_3 were investigated by time-resolved optical absorption spectroscopy using the CO flow-flash technique. The reactions were monitored using multiwavelength detection, which allowed us to resolve the early intermediates, including compound **A**. We demonstrate that ubiquinol/semiquinone plays a complex role in the O_2 reduction mechanism by *E. coli* bo_3, which distinguishes the mechanism of O_2 reduction by bo_3 from the conventional mechanism based on experiments on the bovine enzyme.

MATERIALS AND METHODS

Growth and Purification of bo_3. The wild type bo_3 enzyme was isolated from an *E. coli* strain overexpressing the enzyme (BL21 strain and pET plasmid) and purified as described previously.[19] The enzyme was tagged with a polyhistidine tail for easy isolation by a Ni^{2+}-NTA type column matrix. The final enzyme was solubilized in 50 mM K-phosphate (pH 7.5) chloride-free buffer containing 0.05% *n*-dodecyl-β-D-maltoside detergent (Affymetrix) to ensure that the quinone remained bound to the enzyme. The purified enzyme was characterized by its UV−visible spectra.[10] The amount of ubiquinone-8 in the purified bo_3 preparations was determined by quinone extraction, followed by reversed phase HPLC analysis.[11] The enzyme homogeneity was assessed by heme analysis using a previously described procedure.[11]

Sample Preparation. The reduced enzyme was prepared by taking the oxidized enzyme through alternating cycles of vacuum and nitrogen, followed by the addition of ruthenium hexamine and ascorbic acid (final concentrations of 10 μM and 2 mM, respectively). The fully reduced CO-bound enzyme was attained by incubating the reduced enzyme under CO for 30−60 min.

Time-Resolved Optical Absorption Measurements. The reactions of O_2 and NO with the fully reduced bo_3 were investigated in the presence of CO using the CO flow-flash method.[15] The fully reduced CO-bound enzyme was mixed in a 1:1 ratio with O_2- or NO-saturated buffer, followed by laser photolysis of the CO bound to heme o_3^{2+} with a 532 nm laser pulse from a Q-switched DCR-11 Nd:YAG laser (~7 ns full width at half-maximum).[20]

The time-resolved optical absorption difference spectra (post- minus prephotolysis) were collected at logarithmically spaced delay times from 1 μs to 20 ms. The data were analyzed with singular value decomposition (SVD) and global exponential fitting using programs written in Matlab (Mathworks),[20−23] followed by algebraic kinetic analysis. The validity of a proposed mechanism was judged by the quality of the produced intermediate spectra and their agreement with model spectra when available.

dx.doi.org/10.1021/bi500567m | *Biochemistry* 2014, 53, 5393−5404

RESULTS

Heme and Quinone Analysis. Heme analysis of the purified cytochrome bo_3 preparations resulted in a heme *b*/heme *o* ratio of 1:1, indicating the absence of the cytochrome oo_3 species previously observed in various *E. coli* strains. The quinone content varied between 1.1 and 1.3 quinone/enzyme.

Reaction of the Fully Reduced bo_3 with O_2 Using the CO Flow-Flash Method. The time-resolved optical absorption difference spectra (post- minus prephotolysis) recorded following photolysis of the fully reduced CO-bound wild-type *E. coli* bo_3 in the presence of O_2 are presented in Figure 2. On

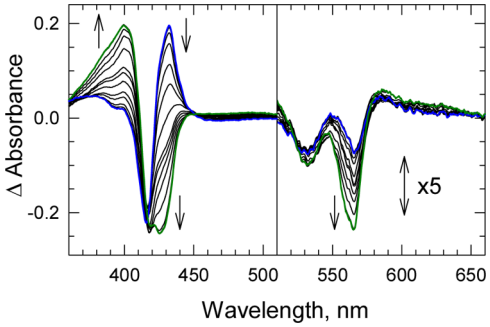

Figure 2. Time-resolved optical absorption difference spectra (post-minus prephotolysis) recorded following photodissociation of the fully reduced CO-bound wild-type *E. coli* bo_3 enzyme in the presence of O_2 (625 μM). The Soret and visible spectra were recorded together at logarithmically spaced time delays between 1 μs and 20 ms. The arrows indicate the direction of change with time. The blue and green traces represent the first (1 μs) and last (20 ms) time points, respectively.

the basis of the assumption that all the processes involved in the O_2 reduction follow first-order kinetics, the data matrix, **A**, can be fitted globally to a sum of time-dependent exponential functions:

$$\mathbf{A} = \sum_i b_i \exp(-r_i t) + \mathbf{R}$$

where r_i are the apparent rate constants and b_i are the pre-exponential factors at each wavelength λ, the so-called *b*-spectra. The fit is considered satisfactory when the matrix of the residuals, **R**, contains only random noise. Direct fitting of the data matrix is cumbersome, and applying singular value decomposition (SVD) to the data matrix greatly simplifies the global exponential fit by reducing the number of time-dependent vectors subject to the fit.[20,22,24] In the SVD analysis, the data matrix is split into three matrices: $\mathbf{A} = \mathbf{U}^*\mathbf{S}^*\mathbf{V}^T$, where the columns of the **U** matrix are the orthonormal basis spectra, and the orthonormal **V** matrix contains the corresponding time-dependent vectors. The diagonal matrix **S** contains the significance values, i.e. the contributions of the *U* and *V* vector pairs to the data. Because there are only a few intermediates involved in the reaction, a limited number of orthogonal *U* and *V* basis vector pairs reproduces the data matrix; the remainder merely represents experimental noise.

On the basis of their significance values and shapes, six *U* and *V* vector pairs were found to contain the kinetic information; the rest, with relative significance below half percent, was regarded as noise. The selected *V* vectors were subject to global exponential fitting using three, four, and five exponential functions. The residuals of the fit, $V - V_{reproduced}$, are shown in Figure 3 together with the level of noise represented by the last six least significant *V* vectors from the SVD. Each curve in

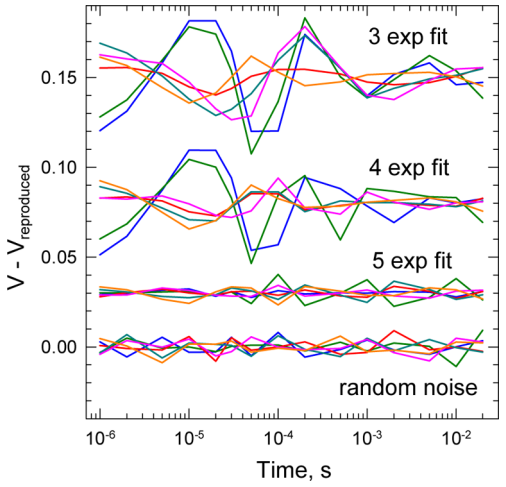

Figure 3. Residuals of three, four, and five exponential fits to time-dependent *V* vectors, namely, $V - V_{reproduced}$, together with the level of noise represented by the last six least significant *V* vectors from the SVD. Each curve is weighted by the corresponding singular value to represent its proper contribution to the data, and each group is displaced for clarity.

Figure 3 is weighted by the corresponding singular value to represent its proper contribution to the data. It is clear that only the combination of five exponential functions reduces the residuals to the experimental noise level. The lifetimes ($1/r_i$) of the five-exponential fit are 22 μs, 30 μs, 42 μs, 470 μs, and 2.0 ms; the three longest lifetimes have been reported previously.[18]

The 22, 30, and 42 μs lifetimes are of primary importance in our effort to resolve the early steps of O_2 reduction by bo_3. These lifetimes are very close in value and, in most cases, fits of this nature cannot be regarded as unique solutions. Indeed, by varying the three lifetimes in this narrow time window, we found other combinations that produced fits with similar residuals. However, while all combinations suggested the same kinetic pattern when analyzed by the technique outlined below, only lifetimes with the average values reported here resulted in acceptable intermediate spectra. The *b*-spectra corresponding to these lifetimes were calculated using the *U* vectors and the results of the five-exponential *V*-vector fit. When lifetimes are as close as the ones reported here, the *b*-spectra become very complex, large in amplitude, and difficult to interpret in terms of transitions between intermediates. Converting the *b*-spectra into intermediate spectra of a unidirectional sequential scheme greatly simplifies the kinetic analysis, and this approach will be followed below.

Deriving the Kinetic Mechanism. The apparent rate constants obtained from the global exponential fit do not represent the actual microscopic rate constants of the reaction steps (except for a unidirectional sequential scheme). Rather, the exponential time dependence observed in a data set is a mathematical consequence of the reaction steps all being first order or pseudo-first order. A proposed mechanistic model connects the apparent rate constants to the microscopic rate constants, and the *b*-spectra to the spectra of the intermediates in the reaction.[20] The mechanism is considered valid if the experimentally derived intermediate spectra have the shapes and amplitudes expected for the intermediates in the scheme or

dx.doi.org/10.1021/bi500567m | *Biochemistry* 2014, 53, 5393−5404

if they can be favorably compared to model spectra available for the respective intermediates. The simplest mechanism is the conventional unidirectional sequential mechanism in which decreasing values of the experimental apparent rate constants, or increasing values of the apparent lifetimes, are assigned to the microscopic rate constants of consecutive steps.

Constructing a mechanism for the reaction of O_2 with *E. coli* bo_3 requires either model spectra of the different bo_3 forms or spectra of intermediates obtained from O_2 reduction experiments on similar well-characterized cytochrome *c* oxidases, such as bovine aa_3 oxidase. In this study, model spectra were linear combinations of the ground-state spectra of the bo_3 in different oxidation and ligation states and, as discussed below, analogous frequency-shifted intermediate spectra of the bovine enzyme. The spectra of compound **A** and the **P** and **F** forms of heme a_3 used in modeling the bo_3 intermediates are derived from the actual intermediate spectra of the bovine enzyme obtained from CO flow-flash experiments.

Intermediate Spectra Based on a Conventional Sequential Mechanism. The intermediate spectra for the reaction of O_2 with fully reduced bo_3 were first determined based on the conventional unidirectional sequential mechanism (Scheme 1), in which increasing lifetimes (decreasing rates) were assigned to consecutive steps.

Scheme 1. Conventional Unidirectional Sequential Mechanism of O_2 Reduction by *E. coli* bo_3

$$\mathbf{R} \xrightarrow{22\,\mu s} \mathbf{Int\ 2} \xrightarrow{30\,\mu s} \mathbf{Int\ 3} \xrightarrow{42\,\mu s} \mathbf{Int\ 4} \xrightarrow{470\,\mu s} \mathbf{Int\ 5} \xrightarrow{2\,ms} \mathbf{Int\ 6}$$

The spectra of the first two intermediates of bo_3 in Scheme 1, **R** (reduced enzyme) and **Int 2**, are shown in Figure 4 (blue curves) together with the corresponding intermediate spectra of the bovine enzyme (Figure 4, green curves). For easier comparison, the amplitudes of all the bovine aa_3 intermediate spectra are normalized based on matching the maximum absorbances of the reduced forms of the two enzymes (Figure 4a). The amplitude difference in the trough of the intermediate difference spectra is attributed to the larger extinction coefficient of the CO-bound bo_3 enzyme, arising from its narrower bandwidth, compared to the CO-bound bovine aa_3 enzyme and will be discussed in more detail below. While the spectrum of the fully reduced intermediate (**R**) of bo_3 (Figure 4a, blue trace) is similar to the analogous intermediate spectrum of the bovine enzyme (Figure 4a, green trace), except for a wavelength shift, it is clear that when the conventional mechanism is applied to the bo_3 data, the shape of the **Int 2** spectrum of the bo_3 (Figure 4b, blue trace), presumed to represent the O_2-bound compound **A** form, is very different from that of the bovine compound **A** spectrum (Figure 4b, green trace). The reason for requiring similar compound **A** spectral shapes for the different enzymes will be addressed below. Judging from its shape alone, **Int 2** of bo_3 in Scheme 1 contains a substantial amount of the reduced form (Figure 4b, blue trace), which could occur if O_2 binding were reversible. Whether this is the case in bo_3 can be tested by using the algebraic kinetic approach we applied previously in our studies of *Thermus thermophilus* ba_3.[20] Introducing reversible O_2 binding, changes the first step in the conventional scheme (Scheme 2).

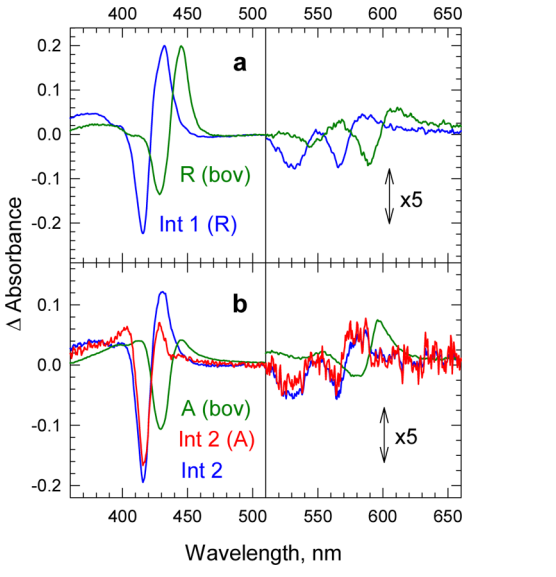

Figure 4. Spectra of the first two intermediates of bo_3 in the conventional (fast-slow) unidirectional sequential O_2 reduction mechanism (Scheme 1), **R** (panel a, blue curve) and **Int 2** (panel b, blue curve) and the corresponding intermediate spectra of the bovine enzyme (green curve). The amplitudes of the bovine aa_3 intermediate spectra are normalized based on matching the maximum absorbances of the reduced forms of the two enzymes in panel a. The red curve in panel b represents the spectrum of compound **A** of bo_3 obtained using the slow-fast mechanism in Scheme 3.

Scheme 2. Reversible O_2 binding

$$\mathbf{R} \underset{k_{21}}{\overset{k_{12}}{\rightleftharpoons}} \mathbf{A} \xrightarrow{k_{23}} \mathbf{X}$$

Our previous analysis of *T. thermophilus* ba_3 showed that the ratio of the observed apparent rates (r_1 and r_2) assigned to the two steps of Scheme 2 restricts the degree of reversibility allowed in the scheme, i.e., the value of $K = k_{12}/k_{21}$ must be larger than its minimal value, $K_{min} = 4\,r_1r_2/(r_1 - r_2)^2$ (for details see ref 20). Considering all the combinations of the three fastest rates (shortest lifetimes), the smallest value for K_{min} is ~8, which corresponds to the 22 and 42 μs lifetime combination; the 22 and 30 μs, and the 30 and 42 μs lifetime combinations both give higher values for K_{min}. A K_{min} value of 8 corresponds to a very forward-shifted equilibrium or practically nonreversible O_2 binding, and it does not support the presence of a large fraction of the reduced form in the second intermediate spectrum of bo_3.

The Slow-Fast Mechanism. The analysis above shows that the difference between the experimental **Int 2** and model compound **A** spectra cannot be explained by the conventional sequential mechanism having a reversible O_2 binding. The algebraic kinetic analysis shows that meaningful spectra of the second and third intermediates in the bo_3 O_2 reaction can only be obtained by using the mechanism in Scheme 3, in which the 42 μs lifetime is assigned to the first step, followed by two faster steps, with lifetimes of 22 and 30 μs. We will refer to this mechanism as the slow-fast mechanism. When a slow step

Scheme 3. Slow-Fast Sequential Mechanism for the Reaction of O_2 with the Fully Reduced *E. coli* bo_3

$$\mathbf{R} \xrightarrow{42\,\mu s} \mathbf{A} \xrightarrow{22\,\mu s} \mathbf{Int\ 3} \xrightarrow{30\,\mu s} \mathbf{Int\ 4} \xrightarrow{470\,\mu s} \mathbf{Int\ 5} \xrightarrow{2\,ms} \mathbf{Int\ 6}$$

dx.doi.org/10.1021/bi500567m | *Biochemistry* 2014, 53, 5393−5404

precedes a faster one in a reaction sequence, it is frequently difficult to isolate the intermediate resulting from the slow step. Nevertheless, using the combination of rates in Scheme 3, we are able to extract the spectra of the previously unresolved intermediates, compound **A** and **Int 3**.

Intermediates 1 and 2. As expected, the experimental spectrum of the first intermediate, the fully reduced enzyme (**R**), determined based on Scheme 3 and referenced versus the fully reduced CO-bound form, is the same as that obtained using the conventional fast-slow mechanism in Scheme 1 (Figure 4a, blue curve).

Figure 4b compares the spectrum of compound **A** of bo_3 obtained using the slow-fast mechanism in Scheme 3 (red trace) and that of **Int 2** of the conventional fast-slow mechanism in Scheme 1 (blue trace) to the bovine $\mathbf{A_R}$ intermediate spectrum (green curve). The spectrum of compound **A** for the bo_3 enzyme produced by the slow-fast mechanism shows none of the reduced form observed when using the conventional (fast-slow) scheme, and the shape of the bo_3 compound **A** (red trace) is similar to that of compound **A** of the fully reduced bovine enzyme (green trace). As noted above, the intensity difference in the trough between the two spectra is due to the higher extinction coefficient of the CO-bound o_3 form than that of the a_3-CO form. The 42 μs lifetime of the first step at 625 μM O_2 corresponds to a second-order rate constant of $\sim 3.8 \times 10^7$ M^{-1} s^{-1} for O_2 binding. This rate is ~2.5 times slower than observed in the bovine and *Rs* aa_3 enzymes, also both of the A-family.

Intermediates 3, 4, 5, and 6. The intermediate formed on the 30−50 μs time scale in the conventional fast-slow unidirectional sequential mechanism for the bovine enzyme is the so-called $\mathbf{P_R}$ intermediate in which heme a_3 is presumed to be in the oxyferryl **P** state and the low-spin heme becomes oxidized. Using the slow-fast mechanism for the reaction of O_2 with reduced bo_3 (Scheme 3), we resolved in addition to compound **A**, two more intermediates in the 20−50 μs time window, **Int 3** and **Int 4**, the spectra of which are shown in Figure 5a and 5b (blue curves), respectively. Using the known heme *b* reduced-minus-oxidized difference spectrum, a good estimate of the heme *b* contribution to the experimental intermediate spectra can be made. Subtracting the respective heme *b* contribution (Figure 5, green curves) from the intermediate spectra yielded the spectra of the heme o_3 in the different intermediates (red curves). These two principal components, heme o_3 and heme *b*, of the intermediate spectra will aid in the derivation of the kinetic mechanism. In the slow-fast mechanism, heme *b* gets completely oxidized in **Int 3**, in contrast to becoming partially oxidized when the traditional fast-slow mechanism is used (not shown). The nature of heme o_3 in **Int 3** will be discussed in more detail below.

The spectrum of **Int 4** is the same irrespective of which one of the two mechanisms, slow-fast or fast-slow, is used. This is expected because **Int 4** is the last member in the chain of the fast (early microsecond) events and it has a relatively long, ~0.5 ms, decay time. The oxidized heme *b* in **Int 3** becomes 60% rereduced during the 30 μs formation of **Int 4**. Heme *a* rereduction in the bovine enzyme is generally associated with the formation of the **F** intermediate and takes place on a significantly longer time scale (~100 μs lifetime).[25−27] In earlier studies of the O_2 reaction in bo_3, only one intermediate was resolved in the 20−50 μs time window.[18] This intermediate was characterized as $\mathbf{P_R}$, the analogue of the bovine $\mathbf{P_R}$ intermediate.

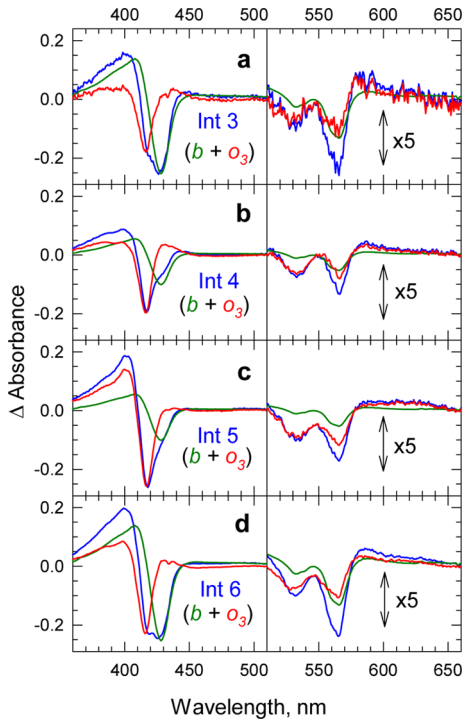

Figure 5. Experimental spectra of intermediates **3**, **4**, **5**, and **6** determined based on the slow-fast unidirectional sequential mechanism in Scheme 3 (blue curves). The spectral contributions of the o_3 reaction center (red curves) and heme *b* (green curves) to the intermediate spectra are shown separately. All the spectra are referenced versus the fully reduced CO-bound enzyme. The heme *b* is fully oxidized in **Int 3**, 60% reduced in **Int 4** and **Int 5**, and fully oxidized in **Int 6**. The contribution of heme o_3 was obtained by subtracting the heme *b* contribution from the corresponding intermediate spectra.

The experimental spectra of **Int 5** and **Int 6** are shown in Figure 5, panels c (blue curve) and d (blue curve), respectively. The level of heme *b* oxidation remains unaltered in the 470 μs transition from **Int 4** to **Int 5** as reflected by the same amplitude of the green curves in Figure 5b and 5c, and complete oxidation of heme *b* is attained only during the 2 ms formation of **Int 6** (Figure 5d, green curve). In earlier studies on the O_2 reaction in bo_3, the end product was formed with a 4 ms lifetime and was assigned to the fully oxidized form, while the preceding intermediate, produced with 700 μs lifetime, was attributed to the partial reduction of heme *b* by the ubiquinol.[18] A brief comparison of the amplitudes of the o_3 spectral contributions in **Int 5** and **Int 6** at 400 nm, the wavelength at which the absorbance is mostly due to the oxidized o_3 form (Figure 5c and 5d, red curves), shows that **Int 5** is more likely to be the oxidized form of o_3 than **Int 6**. From the brief description of the intermediates above, it is clear that we cannot draw a direct analogy between the kinetics of the bovine enzyme and that of bo_3.

Reaction of Fully Reduced Wild-Type bo_3 with NO. In order to confirm the assignment of the 40 μs lifetime to the O_2 binding step, we investigated the binding of NO, a substrate analogue for O_2, to heme o_3^{2+}. NO binds to the bo_3 enzyme without subsequent redox chemistry, which allows us to determine the rate of ligand binding accurately and unambiguously. Although bo_3 does have some NO reductase activity, the reduction of NO to N_2O takes place on millisecond

dx.doi.org/10.1021/bi500567m | *Biochemistry* 2014, 53, 5393−5404

time scale,[4] and thus it does not interfere with the much faster binding process reported here.

The time-resolved difference spectra (post- minus prephotolysis) following photolysis of the fully reduced CO-bound bo_3 enzyme in the presence of NO (50% saturated NO solution; 0.9 mM after mixing) are presented in Figure 6a. The SVD-based global exponential fitting resolved one lifetime of 33 μs; the corresponding *b*-spectra are shown in Figure 6b. The single lifetime of 33 μs at 0.9 mM NO concentration in the presence of CO (0.6 mM) is attributed to NO binding based on the corresponding *b*-spectrum (blue trace), which has the shape of the difference spectrum between the reduced and NO-bound forms of bo_3. This lifetime corresponds to a second-order rate constant of $\sim 3.4 \times 10^7$ M^{-1} s^{-1} for NO binding, which is the same within experimental error as found for O_2 binding ($\sim 3.8 \times 10^7$ M^{-1} s^{-1}) using the slow-fast mechanism.

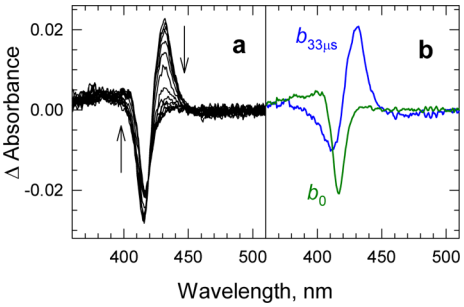

Figure 6. (a) Time-resolved optical absorption difference spectra (post- minus prephotolysis) of the reaction of fully reduced *E. coli* bo_3 with NO following photolysis of the CO-bound enzyme. The Soret and visible spectra were recorded at 15 delay time points, logarithmically spaced between 0.2 μs to 10 ms. The NO concentration after mixing was 0.9 mM. (b) *b*-spectra resulting from a single-exponential fit of the time-resolved optical absorption difference spectra. The blue curve shows the spectral change corresponding to the 33 μs lifetime, and the green curve (b_0) represents the spectrum extrapolated to infinite time.

DISCUSSION

The early flow-flash studies on the reaction of O_2 with the fully reduced *E. coli* bo_3 were complicated by the observation of different types of kinetics, monophasic versus multiphasic, depending on the isolation procedure and the strain used for the overexpression of the enzyme.[8,17] In the current work, the quality of the isolated *E. coli* bo_3 is improved over that used in previous studies so that the heme content is consistently 1 heme *b*/1 heme o_3 and there is no oo_3 species present. While the monophasic kinetics obtained in previous studies could be attributed to the ubiquinone-depleted enzyme and the multiphasic kinetics to the ubiquinone-bound enzyme,[8] the binding of O_2 to the heme o_3 was not resolved, and the spectra of the intermediates were not determined. To successfully address this issue, we collected absorption spectra over a broad wavelength range and in a wide time window. Combining this data collection with a rigorous algebraic kinetic analysis allowed us to derive the complete kinetic mechanism for the O_2 reduction by bo_3, which involves an unusual combination of fast reaction rates that could not be resolved earlier.

As discussed above, the first step in our strategy for resolving the chemistry in the kinetic steps of the O_2 reaction in *E. coli* bo_3 was the separation of the contributions made by heme *b* and the o_3 reaction center to the intermediate spectra. The second step, addressed below, involves identifying the state of the o_3 reaction center in the intermediates. To accomplish this goal, we rely on the known spectral shapes of the bovine a_3 reaction center in its different states, including compound **A**, and **P** and **F**. For a direct comparison of the spectra of the o_3 and a_3 forms, we developed the spectral-shift method outlined below.

Modeling the bo_3 Enzyme Intermediates with Bovine Enzyme Intermediate Spectra. The spectra of the o_3 reaction center in *E. coli* bo_3 and a_3 in the bovine enzyme cannot be overlaid by shifting one spectrum on the wavelength scale because the bovine aa_3 absorbance spectra are red shifted by ~25 nm in the visible region and by ~13 nm in the Soret region relative to the o_3 spectra (Figure 4). However, the spectral forms of heme o_3 compare favorably with those of heme a_3 after shifting the latter on the energy or frequency scale. This energy scale shift compensates for the difference in energy gap between the electronic states of the two hemes while leaving the shape of the energy distribution unaltered. The net effect of applying the energy scale approach is a blue shift of the bovine spectra, the extent of which depends on the λ_{max} of the bands, and some narrowing of the shifted bands when visualized on the wavelength scale. This technique was tested on the reduced-minus-reduced-CO difference spectra of heme a_3 and heme o_3. As expected and shown in Figure 7a, shifting the a_3 spectrum on the energy scale results in different shifts of the absorption maxima in the Soret region versus those in the visible region when viewed on the wavelength scale, resulting in a reasonable match between the positions of the peaks in the spectra of the two enzymes in both spectral regions. Applying the same amount of energy shift also results in a good agreement between the absorption maxima of the oxidized a_3 and o_3 absorption spectra and, as illustrated below,

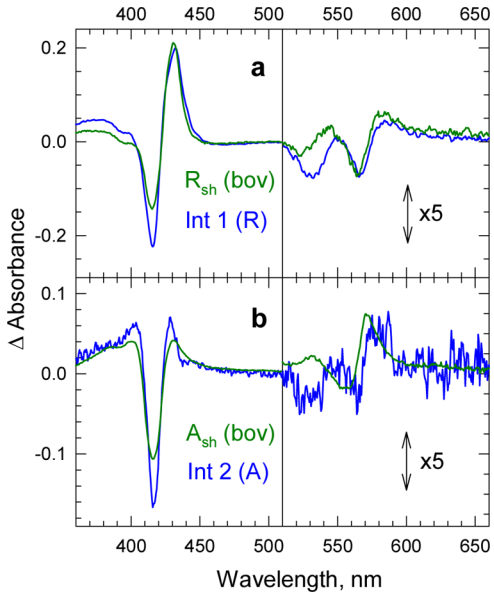

Figure 7. (Blue curves) The experimental spectra of **Int 1** (**R**) (a) and **Int 2** (**A**) (b) in the reaction of reduced bo_3 with O_2 in the slow-fast mechanism in Scheme 3. (Green curves) The frequency-shifted spectra of the reduced enzyme, $\mathbf{R_{sh}}$, and compound **A** ($\mathbf{A_{sh}}$) obtained from a CO flow-flash experiment on the reaction of the reduced bovine enzyme with O_2. The spectra are all referenced versus the respective fully reduced CO-bound enzyme.

dx.doi.org/10.1021/bi500567m | *Biochemistry* 2014, 53, 5393−5404

this is also the case for other known intermediates generated during the O_2 reaction.

Compound A. The mechanism of the reduction of dioxygen to water in *E. coli* bo_3 has been postulated to be analogous to the mechanism commonly proposed for the bovine heart enzyme (Scheme 1) based on previous CO flow-flash studies of the fully reduced bo_3.[8,18] An apparent lifetime of 27 μs at 1.25 mM O_2 was attributed to O_2 binding to fully reduced bo_3,[16] which corresponds to a second-order rate constant of 3×10^7 M^{-1} s^{-1}; the same O_2 binding rate was observed for the chloride-treated enzyme (monophasic kinetics and presumably ubiquinone-depleted enzyme) and the sulfate-treated enzyme (multiphasic kinetics and ubiquinone-containing enzyme). The spectrum of compound **A** was not resolved at room temperature, and the O_2 binding was postulated to be a rate-limiting step in the dioxygen reduction.[16]

Our kinetic analysis that produced the slow-fast mechanism does show that the O_2 binding is rate limiting for the subsequent electron transfer process, and using this scheme also allowed us to extract the spectrum of compound **A**. However, it should be noted that in our search for the proper scheme, we required that the spectrum of the second intermediate be similar in shape to that of compound **A** of the bovine enzyme. This requirement is not without merit as it is based on the general trend seen in the spectra of the high-spin heme in the heme-copper oxidases interacting with dioxygen/oxygen in different forms, particularly those of compound **A**, **P**, and **F** states. The strongly allowed Soret transitions of **A**, **P**, and **F** all have practically the same λ_{max}, spectral widths, and extinction coefficients. When the high-spin heme interacts with CO, the λ_{max} of the Soret transition is practically the same as for the **A**, **P**, and **F** forms. However, the bandwidth becomes smaller and the peak extinction coefficients of the CO-bound forms are somewhat larger, suggesting that the oscillator strength is similar to that of **A**, **P**, and **F**. As a result, when the spectrum of compound **A** is referenced against the respective CO-bound form, the difference spectrum shows only a trough with a small hump on either side (Figure 7b). The depth of the trough and the height of the humps depend on how narrow the spectrum of the reduced CO-bound enzyme is relative to that of the O_2-bound state. The spectrum of the CO-bound form of heme o_3 is apparently narrower than that of heme a_3; hence the trough in the compound **A**-minus-reduced-CO difference spectrum of o_3 is deeper, and the humps are somewhat taller than seen in the corresponding a_3 difference spectrum (Figure 7b, blue and green curves, respectively). As shown below, the same argument applies to the difference spectra of **P** and **F** (referenced against the CO-bound form).

The difference spectrum of the bo_3 compound **A** in our study is very similar to the first spectrum recorded following photolysis of fully reduced CO-bound cytochrome bo_3 in membrane suspensions in the presence of O_2 at −80 °C; in this first difference spectrum (0.1 min after photolysis), the 430 nm peak due to the reduced heme o_3 has decayed as a result of O_2 binding.[28] Time-resolved resonance Raman studies on the reaction of reduced *E. coli* bo_3 with O_2 indicated the accumulation of compound **A** between ∼0−20 μs at 5 °C based on a stretching frequency of 568 cm^{-1}.[29]

The Nature of Int 3 and Int 4. To identify the state of heme o_3 in the bo_3 **Int 3** and **Int 4** in Scheme 3, the respective o_3 spectra, without the spectral contributions of heme *b*, are shown in Figure 8a and 8b (blue curves), together with the

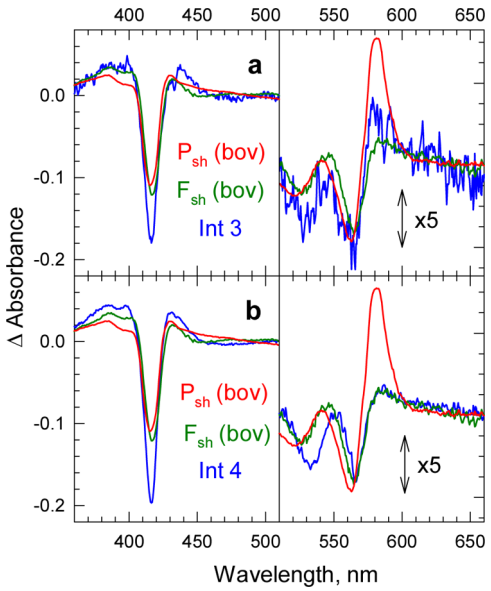

Figure 8. (Blue curves) The experimental spectra of heme o_3 in **Int 3** (a) and **Int 4** (b) in the slow-fast mechanism (Scheme 3). (Red and green curves) The frequency-shifted bovine **P** ($\mathbf{P_{sh}}$) and **F** ($\mathbf{F_{sh}}$) spectral forms, respectively, obtained from a CO flow-flash experiment on the reaction of the bovine enzyme with O_2. The spectra are referenced versus the corresponding reduced CO-bound enzyme.

frequency-shifted bovine **P** and **F** spectral forms (red and green curves, respectively). It is clear that **Int 3** in the bo_3 enzyme (Figure 8a, blue) does not match the frequency-shifted **P** form of the bovine enzyme in the more characteristic visible region (Figure 8a, red) and that there appears to be a better agreement with the frequency-shifted **F** form (Figure 8a, green). However, considering the small accumulation of **Int 3** and its minor contribution to the recorded spectra (as reflected by the rather low signal-to-noise ratio), it cannot be stated with certainty that a small fraction of the bo_3 **Int 3** is not **P**. Moreover, this comparison assumes that the bovine aa_3 **P** and **F** forms are good representatives of the analogous states of bo_3. The fraction of **P** in **Int 3**, which we estimate to be ∼30%, could be larger or smaller depending on the exact spectral shape of the **P** form of the bo_3.[30,31] The much more accurate **Int 4** spectrum is in very good agreement with the frequency-shifted bovine **F** form, particularly in the less precise but more characteristic visible region (Figure 8b). It is safe to conclude that the intermediate we observe at the end of the early microsecond time scale, ∼ 50 μs, is not a **P** but rather an **F** form.

The observation that compound **A** is converted rapidly to an **F**-like intermediate differs from recent findings on the dioxygen reduction mechanism in *T. thermophilus* ba_3, which does not include the 580 nm **F** state.[20,32,33] The results reported here are more in line with multiwavelength time-resolved optical absorption studies on the bovine enzyme in our laboratory, which showed that $\mathbf{P_R}$ is not a pure **P** form but rather a mixture of the **P**, **F**, and compound **A** forms.[23] Moreover, recent time-resolved optical absorption studies on *R. sphaeroides* aa_3 in our laboratory demonstrated that at least at neutral pH (7.4) $\mathbf{P_R}$ is not observed in the O_2 reduction mechanism of this enzyme and that compound **A** is converted to the **F** intermediate.[34] The failure to detect **P** during O_2 reduction in *R. sphaeroides* aa_3[34] and the observation of a limited **P** fraction in *E. coli* bo_3 (current study) do not necessarily invalidate a hypothetical mechanism that includes a very short-lived **P**-like intermediate state. The

dx.doi.org/10.1021/bi500567m | *Biochemistry* 2014, 53, 5393−5404

short lifetime of **P** might arise from very fast proton transfer, leading to nearly instantaneous conversion of **P** to **F**, compared to slower electron transfer from the low-spin heme to the binuclear site.[34] Time-resolved resonance Raman experiments identified an oxyferryl **F** intermediate during the reaction of reduced *E. coli* bo_3 with O_2 based on a stretching frequency of 788 cm^{-1},[29] which is close to the frequency reported for the oxyferryl **F** intermediate of the bovine enzyme (785 cm^{-1});[35−37] the 788 cm^{-1} band in *E. coli* bo_3 has been correlated with the 557 nm absorption band of the oxyferryl **F** state.[38] Importantly, the rise time of the oxyferryl **F** intermediate of the bo_3 quinol oxidase (~20−40 μs at 5 °C) was found to be significantly faster than that of the bovine enzyme under similar conditions, which is in accordance with the accelerated formation of the oxyferryl, **F**, intermediate reported here. In the bovine enzyme, two oxygen-sensitive bands identified at 804 and 786 cm^{-1} during the reaction of O_2 with the reduced enzyme were attributed to **P** and **F**, respectively.[39] The former was not observed in the *E. coli* bo_3 enzyme.[29]

The spectrum of **Int 4** generated on ~30 μs time scale (Figure 5b, blue curve) shows substantial, ~60%, reduction of the low-spin heme *b*, with heme o_3 being in the **F** state. The electron donor to heme *b* is assumed to be the ubiquinol, producing semiquinone. The electron transfer from ubiquinol to heme *b* observed here is significantly faster than reported earlier (~700 μs).[18]

Intermediate 5. The spectral amplitude of heme o_3 in **Int 5** (Figure 5c, red curve) is the largest among all the intermediates around 400 nm where the oxidized heme o_3 absorbs. This strongly suggests that the 470 μs process involves the conversion of the o_3 **F** state in **Int 4** to the o_3 oxidized **O** state in **Int 5** and, significantly, that this conversion occurs *without* the simultaneous oxidation of the reduced heme *b*. This conclusion is supported by Figure 9a, which shows the difference between the experimental **Int 4** and **Int 5** spectra (blue curve), the difference between the bovine frequency-shifted **F** and **O** forms (green curve) and the bench-made difference spectrum between the o_3 **F** and the oxidized o_3^{3+} forms obtained from the reaction of the oxidized bo_3 with H_2O_2 at pH 9 (red curve). It is postulated that the electron required to convert the oxyferryl o_3 **F** state to the oxidized o_3^{3+} state is supplied by the semiquinone/ubiquinol mixture present. Whether the electron is donated directly to heme o_3 or indirectly via heme *b* is an open question. The choice of path depends on the detailed structure of the energy landscape separating the electron donor from the acceptor. The timing of the 470 μs process may be linked to and controlled by the rate of proton transport in the protein similar to that reported for the final oxidation step in the bovine enzyme.[40,41] Previous flow-flash studies of the reaction of fully reduced bo_3 with O_2 indicated proton release on the 550 μs time scale.[18]

Intermediate 6. A comparison of the green curves in Figure 5c and 5d shows that the final step in the mechanism involves the complete oxidation of heme *b* with 2 ms lifetime. Concomitantly, the reduction in amplitude of the o_3 form around 400 nm in Figure 5d as compared to Figure 5c (red curves) indicates that the oxidized o_3 in **Int 5** becomes partially rereduced in **Int 6** and, following O_2 binding, regenerates a form, which is apparently very similar to that of **Int 3**. This is reflected in Figure 9b, which shows the difference spectrum between the final intermediate, **Int 6**, and **Int 5** (blue curve), and 60% of the difference spectrum between **Int 3** and **Int 5**

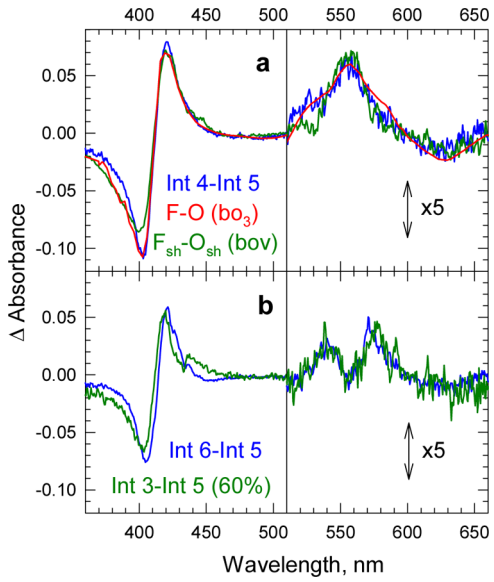

Figure 9. (a) The difference between the bo_3 experimental spectra of **Int 4** and **Int 5** (blue curve), the difference between the bovine aa_3 frequency-shifted **F** and **O** spectral forms ($\mathbf{F_{sh}} - \mathbf{O_{sh}}$; green curve) and the bench-made difference spectrum between the o_3 **F** and the oxidized o_3^{3+} forms obtained from the reaction of the oxidized bo_3 with H_2O_2 at pH 9 (red curve). (b) The difference spectrum between the final bo_3 intermediate, **Int 6**, and **Int 5** (blue curve), and the 60% of the difference spectrum between the bo_3 **Int 3** and **Int 5** (green curve) after subtracting the heme *b* contribution from each of the intermediate spectra involved.

(green curve) after subtracting the heme *b* contribution from each of the intermediate spectra involved. It should be noted that the shape of the difference spectra in the visible region suggests that some **P** is present in both **Int 3** and **Int 6**. The source of every electron necessary (1.2 electron equivalents) for the partial rereduction of the binuclear reaction center is not known. A total of one electron could come from heme *b* (0.6) and the semiquinone (0.4) and the remainder could originate from ubiquinol present in the sample in excess of 1 equiv of quinone/enzyme, i.e., at the Q_L site, and be mediated to the binuclear site through the Q_H site; the rate of electron transfer from the Q_L site to Q_H does not appear to be a limiting factor. The extra electron equivalent (0.6) required to split the O_2 bound to the o_3 center may originate from Q_L, if present in sufficient amount. The cross-linked tyrosine may also serve as an electron donor.

The Molecular Mechanism. On the basis of the analysis above, we propose the mechanism in Scheme 4 (top) for the reduction of dioxygen to water in *E. coli* bo_3. Scheme 4 (middle) represents possible intermolecular electron shuffling on early millisecond time scale funneling the available electrons to a fraction of the molecules, creating 60% of the transient partially reduced form ($\mathbf{R_M}$) and 40% of the oxidized form. While the electrons in the $\mathbf{R_M}$ state are expected to be redistributed among the redox centers according to their electrochemical potentials, for simplicity, the electrons are assigned to the binuclear center, which generates the equivalent of a "mixed-valence" reduced state.

The bottom part of Scheme 4 shows a plausible route from the transient $\mathbf{R_M}$ state (60% of the original enzyme population) to the observed **P**/**F** intermediate during the second turnover cycle. Because our enzyme preparations contain between 1.1

dx.doi.org/10.1021/bi500567m | *Biochemistry* 2014, 53, 5393−5404

Scheme 4. Proposed Mechanism for the O_2 Reduction in *E. coli* bo_3[a]

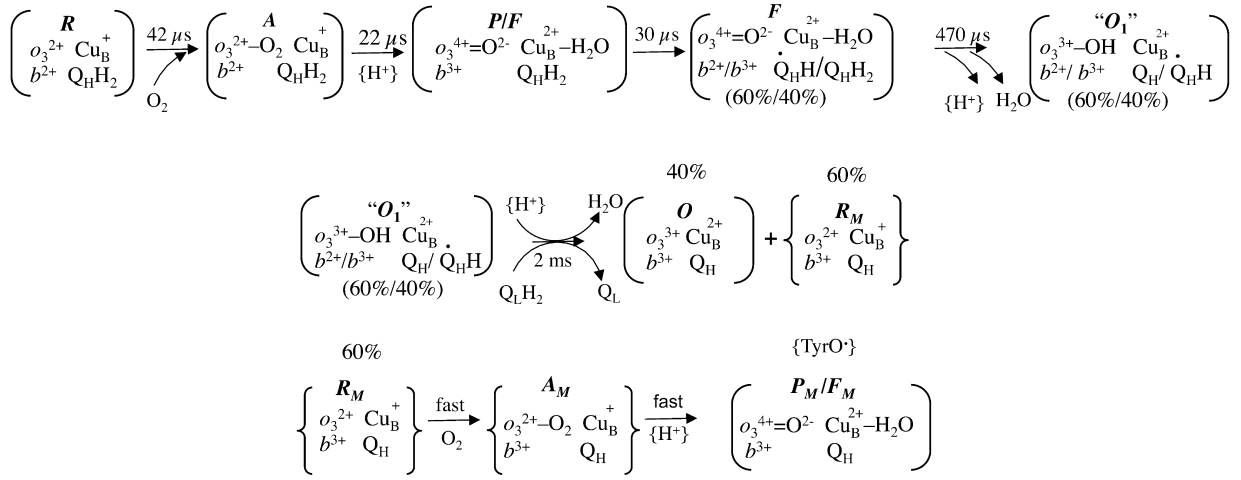

[a]The [ ] are "observed" intermediates proposed based on the correspondence between the experimental and model spectra while the { } intermediates are not observed but represent plausible transient states. The {TyrO·} is the cross-linked tyrosine radical, and the {H^+} can represent either internal or external proton release/uptake. The semiquinone is shown in a neutral form.[42]

and 1.3 ubiquinone/enzyme, the extra electron equivalent (~0.6 in the above scheme) required to break the O−O bond during the second cycle is postulated to come from the cross-linked tyrosine.

Figure 10 shows the concentration profiles of the intermediates in the slow-fast mechanism (Scheme 4) as a function of time. Although the 42 μs O_2 binding is followed by two faster steps, a small, but still observable, accumulation of the previously undetected compound **A** is predicted and indeed resolved. Despite the similar accumulation of compound **A** and **P**/**F**, it is much more difficult to resolve the latter than the former because of the almost identical absorption spectra of the "oxygen-bound" **A**, **P**, and **F** forms in the Soret region, the spectral region that drives the global exponential fit due to its high extinction coefficients. Because heme *b* oxidation in **P**/**F** is quickly followed by its rereduction, the spectral contribution coming from heme *b* is on the borderline of the detection limit.

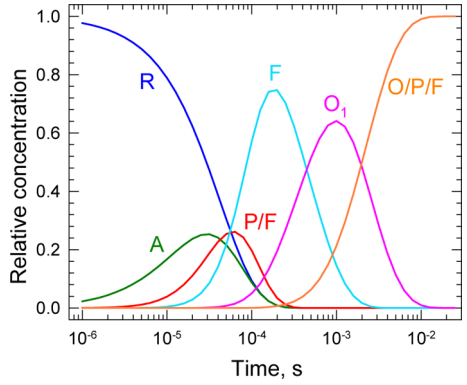

Figure 10. Concentration profiles of the intermediates in the slow-fast mechanism (Scheme 4) as a function of time.

Role of Ubiquinol/Semiquinone in the Catalytic Mechanism. The involvement of ubiquinol and semiquinone in the O_2 reduction mechanism described above is supported by previous studies. Cytochrome bo_3 displays a semiquinone EPR signal when the enzyme is partially reduced.[43,44] The stabilization of the one-electron reduced form at the high affinity site (Q_H) is consistent with the ubiquinone at this site being capable of being reduced by two electrons, and subsequently transferring the electrons one at a time to an electron acceptor, which is considered to be heme *b*.[11] Rapid freeze-quenching EPR experiments have also indicated that semiquinone formed at the Q_H site is an intermediate in the catalytic reduction of dioxygen to water by bo_3.[45] Furthermore, the generation of semiquinone in *E. coli* bo_3 has been demonstrated by pulse radiolysis, using *N*-methylnicotinamide as a mediator.[46] Following the 10 μs formation of the semiquinone after pulse radiolysis, the semiquinone in turn reduced both heme *b* and heme o_3 with a first-order rate constant of 1.5×10^3 s^{-1} (670 μs). Significantly, this lifetime is quite similar to the 500 μs lifetime observed in our study, which we attribute to electron transfer primarily from the semiquinone to the o_3 **F** form. As mentioned above, the electron from the semiquinone could be donated directly to the o_3 reaction center or indirectly via heme *b*. The authors of the pulse radiolysis study concluded that the reduction of the hemes must take place through heme *b*, which would subsequently transfer the electron to heme o_3 until equilibrium was reached between the two hemes;[46] fast electron transfer (~3 μs) from heme o_3 to heme *b* has been reported in reverse electron transfer studies on the mixed-valence CO-bound bo_3 enzyme.[47]

Electron Transfer Rate between Ubiquinol and Heme *b*. Earlier studies suggested that the 700 μs lifetime observed during O_2 reduction by bo_3 represented electron transfer from the ubiquinol to heme *b*,[18] while our results indicate a significantly faster rate of 30 μs. We can estimate the rate of electron transfer between the ubiquinol and heme *b* using the semiclassical electron transfer theory formulated by Marcus and Sutin.[48] The theory expresses the rate constant for electron transfer between a donor and acceptor at a fixed distance and orientation in terms of three parameters: the driving force for electron transfer, $-\Delta G^o$, a reorganization parameter, λ, and the electron coupling (H_{AB}) between the two redox centers at the nuclear orientation of the transition state.[49] On the basis of modeling the ubiquinone-2 into the proposed Q_H ubiquinone binding site as postulated by Abramson et al.,[5] we find that the

dx.doi.org/10.1021/bi500567m | *Biochemistry* 2014, 53, 5393−5404

shortest route between the ubiquinone and heme *b* is through His106, Ile102, and His98 and involves 14 covalent bonds and 3 H-bonds (total distance of ~26 Å) (Figure 11). Previous

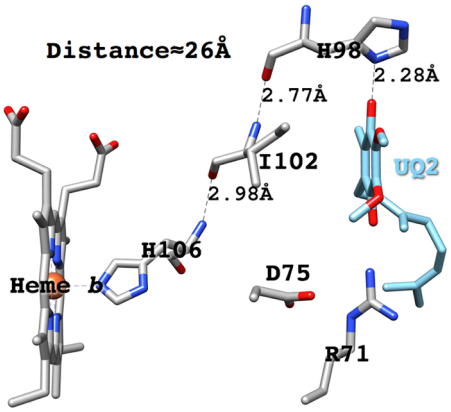

Figure 11. Shortest electron transfer pathway connecting the ubiquinol to heme *b*. The 26 Å route involves 14 covalent bonds and 3 hydrogen bonds.

studies have shown that the driving-force-optimized protein tunneling depends exponentially on the distance with $H_{AB} = H^0_{AB}e^{-\beta(r-r_0)/2}$, which yields an electron transfer rate at close contact (r_0 = 3 Å) of 10^{13} s^{-1}, and H^0_{AB} of 0.0231 eV.[50] Using a distance decay constant β of 1.1 $Å^{-1}$, based on the similarity of our pathway to that estimated for Ru-modified proteins such as azurins,[51,52] r = 16 Å for the distance between Fe of heme *b* and the center of ubiquinone-2,[5] $-\Delta G^0$ of 0.04 eV at pH 7.5 ($\Delta E^0 = E^0(b^{3+/2+}) + E^0(QH_2/Q\cdot) = 0.123-0.082 = 0.041$ eV[44,45]), λ of 0.6 eV (most reorganization energies for biological electron transfer reactions vary between 0.6 and 0.8), we determined the rate of electron transfer from ubiquinol to the Fe of heme *b* to be 4.2×10^4 s^{-1} or 24 μs, which is in good agreement with the rate of 30 μs observed in our experiment. It should be noted that the experimental rate constant for electron transfer from Cu_A to cytochrome *a* in cytochrome *c* oxidase is similar to that reported here, ~50 μs.[23,24,53] Moreover, the direct electron transfer pathway from Cu_A to heme *a* involves 14 covalent bonds (the same as we postulate for the electron transfer from ubiquinol to heme *b*) and 2 hydrogen bonds, with an effective tunneling length of 25.2 Å; a reorganization energy, λ, between 0.5 and 0.6 eV was found to reproduce the experimental rate for the bovine enzyme.[54] Preliminary results in our laboratory on the ubiquinone-depleted cytochrome bo_3 support our conclusions of rapid (30 μs) electron injection by the bound quinol. Some of the discrepancies between our kinetic O_2 reduction mechanism in *E. coli* bo_3 and the conventional one reported earlier,[18] namely, the rate of heme *b* rereduction and the involvement of ubiquinol in both early and late steps, may be due to differences in the ubiquinone content of the bo_3 samples used in the two experiments.

CONCLUSIONS

Several important findings have resulted from our studies. First, we have resolved the spectrum of the O_2-bound intermediate, compound **A**, in the mechanism of O_2 reduction by *E. coli* bo_3 using an algebraic kinetic approach and demonstrated directly that the O_2 binding is indeed rate limiting for the subsequent electron transfer process. Strong support for our slow-fast mechanism comes from a comparison of the O_2 and NO experiments, which give the same second-order rate constants of ligand binding only when the 42 μs lifetime is assigned to O_2 binding, and is followed by two faster steps. Second, compound **A** decays to the **F** form, through a short-lived mixture of **P** and **F** intermediates, on the 30 μs time scale, which is generally attributed to the $\mathbf{P_R}$ formation in the bovine enzyme. Third, the rereduction of heme *b*, presumably through electron transfer from the bound ubiquinol to generate semiquinone, occurs with a lifetime of 30 μs, which is significantly faster than the 700 μs lifetime reported earlier.[18] Fourth, the 470 μs process involves the conversion of the o_3 **F** form to the fully oxidized state, o_3^{3+}, by semiquinone/ubiquinol, while heme *b* does not change redox state. Hence the ubiquinol and semiquinone appear to be involved in electron transfer chemistry on both the early and late microsecond time scales in the O_2 reduction reaction. Fifth, the final millisecond process involves the reoxidation of heme *b* as well as partial rereduction of the binuclear center and, following O_2 binding, the formation of an o_3 oxy-ferryl **P**/**F** intermediate. The role ubiquinol plays in bo_3 O_2 reduction kinetics is clearly more complex than previously thought, and determination of the molecular structures of the Q_H and Q_L sites should help gain additional insight into the intramolecular electron transfer in this enzyme.

AUTHOR INFORMATION

Corresponding Author

*E-mail: olof@ucsc.edu. Fax: (831) 459-2935. Phone: (831) 459-3155.

Present Addresses

[#]Physical Biosciences Division, Lawrence Berkeley National Laboratory, Berkeley, CA.

[⊥]Department of Chemistry, University of Oregon, Eugene, OR 97403.

Funding

This work was supported by the National Science Foundation Grant CHE-1158548 (Ó.E.) and by DE-FG02−87ER13716 (R.B.G.) from the Chemical Sciences, Geosciences and Biosciences Division, Office of Basic Energy Sciences, Office of Sciences, United States Department of Energy.

Notes

The authors declare no competing financial interest.

ACKNOWLEDGMENTS

We thank Harry Gray and Kana Takematsu for helpful discussions.

ABBREVIATIONS

SVD, singular value decomposition; *b*-spectrum, spectral changes associated with an apparent rate (lifetime); Q_H, high-affinity ubiquinone binding site; Q_L, low-affinity ubiquinone binding site; QH_2, ubiquinol; $\dot{Q}_HH$, semiquinone at the Q_H site; Q, ubiquinone

REFERENCES

(1) Mogi, T., Tsubaki, M., Hori, H., Miyoshi, H., Nakamura, H., and Anraku, Y. (1998) Two terminal quinol oxidase families in *Escherichia coli*: variations on molecular machinery for dioxygen reduction. *J. Biochem. Mol. Biol. Biophys. 2*, 79−110.

(2) Pereira, M. M., Santan, M., and Teixeira, M. (2001) A novel scenario for the evolution of haem-copper oxygen reductases. *Biochim. Biophys. Acta 1595*, 185−208.

(3) Puustinen, A., Finel, M., Virkki, M., and Wikström, M. (1989) Cytochrome *o* (*bo*) is a proton pump in *Paracoccus denitrificans* and *Escherichia coli*. *FEBS Lett. 249*, 163−167.
(4) Butler, C. S., Forte, E., Scandurra, F. M., Arese, M., Giuffrè, A., Greenwood, C., and Sarti, P. (2002) Cytochrome bo_3 from *Escherichia coli*: the binding and turnover of nitric oxide. *Biochem. Biophys. Res. Commun. 296*, 1272−1278.
(5) Abramson, J., Riistama, S., Larsson, G., Jasaitis, A., Svensson-Ek, M., Laakkonen, L., Puustinen, A., Iwata, S., and Wikström, M. (2000) The structure of the ubiquinol oxidase from *Escherichia coli* and its ubiquinone binding site. *Nat. Struct. Biol. 7*, 910−917.
(6) Tsukihara, T., Aoyama, H., Yamashita, E., Tomizaki, T., Yamaguchi, H., Shinzawa-Itoh, K., Nakashima, R., Yaono, R., and Yoshikawa, S. (1996) The whole structure of the 13-subunit oxidized cytochrome *c* oxidase at 2.8 Å. *Science 272*, 1136−1144.
(7) Wu, W., Chang, C. K., Varotsis, C., Babcock, G. T., Puustinen, A., and Wikström, M. (1992) Structure of the heme *o* prosthetic group from the terminal quinol oxidase of *Escherichia coli*. *J. Am. Chem. Soc. 114*, 1182−1187.
(8) Puustinen, A., Verkhovsky, M. I., Morgan, J. E., Belevich, N. P., and Wikström, M. (1996) Reaction of the *Escherichia coli* quinol oxidase cytochrome bo_3 with dioxygen: the role of a bound ubiquinone molecule. *Proc. Natl. Acad. Sci. U.S.A. 93*, 1545−1548.
(9) Sato-Watanabe, M., Mogi, T., Miyoshi, H., Iwamura, H., Matsushita, K., Adachi, O., and Anraku, Y. (1994) Structure-function studies on the ubiquinol oxidation site of the cytochrome *bo* complex from *Escherichia coli* using p-benzoquinones and substituted phenols. *J. Biol. Chem. 269*, 28899−28907.
(10) Sato-Watanabe, M., Mogi, T., Ogura, T., Kitagawa, T., Miyoshi, H., Iwamura, H., and Anaraku, Y. (1994) Identification of a novel quinone-binding site in the cytochrome *bo* complex from *Escherichia coli*. *J. Biol. Chem. 269*, 28908−28912.
(11) Yap, L. L., Lin, M. T., Ouyang, H., Samoilova, R. I., Dikanov, S. A., and Gennis, R. B. (2010) The quinone-binding sites of the cytochrome bo_3 ubiquinol oxidase from *Escherichia coli*. *Biochim. Biophys. Acta 1797*, 1924−1932.
(12) Einarsdóttir, Ó. (1995) Fast reactions of cytochrome oxidase. *Biochim. Biophys. Acta 1229*, 129−147.
(13) Einarsdóttir, Ó., and Szundi, I. (2004) Time-resolved optical absorption studies of cytochrome oxidase dynamics. *Biochim. Biophys. Acta 1655*, 263−273.
(14) Ferguson-Miller, S., and Babcock, G. T. (1996) Heme/copper terminal oxidases. *Chem. Rev. 96*, 2889−2907.
(15) Gibson, Q. H., and Greenwood, C. (1963) Reactions of cytochrome oxidase with oxygen and carbon monoxide. *Biochem. J. 86*, 541−554.
(16) Orii, Y., Mogi, T., Kawasaki, M., and Anraku, Y. (1994) Facilitated intramolecular electron transfer in cytochrome *bo*-type ubiquinol oxidase initiated upon reaction of the fully reduced enzyme with dioxygen. *FEBS Lett. 352*, 151−154.
(17) Orii, Y., Mogi, T., Sato-Watanabe, M., Hirano, T., and Anraku, Y. (1995) Facilitated intramolecular electron transfer in the *Escherichia coli bo*-type ubiquinol oxidase requires chloride. *Biochemistry 34*, 1127−1132.
(18) Svensson Ek, M., and Brzezinski, P. (1997) Oxidation of ubiquinol by cytochrome bo_3 from *Eschericia coli*: kinetics of electron and proton transfer. *Biochemistry 36*, 5425−5431.
(19) Frericks, H. L., Zhou, D. H., Yap, L. L., Gennis, R. B., and Rienstra, C. M. (2006) Magic-angle spinning solid-state NMR of a 144 kDa membrane protein complex: *E. coli* cytochrome bo_3 oxidase. *J. Biomol. NMR 36*, 55−71.
(20) Szundi, I., Funatogawa, C., Fee, J. A., Soulimane, T., and Einarsdóttir, Ó. (2010) CO impedes superfast O_2 binding in ba_3 cytochrome oxidase from *Thermus thermophilus*. *Proc. Natl. Acad. Sci. U.S.A. 107*, 21010−21015.
(21) Hug, S. J., Lewis, J. W., Einterz, C. M., Thorgeirsson, T. E., and Kliger, D. S. (1990) Nanosecond photolysis of rhodopsin: Evidence for a new, blue-shifted intermediate. *Biochemistry 29*, 1475−1485.
(22) Szundi, I., Lewis, J. W., and Kliger, D. S. (1997) Deriving reaction mechanisms from kinetic spectroscopy. Application to late rhodopsin intermediates. *Biophys. J. 73*, 688−702.
(23) Szundi, I., Van Eps, N., and Einarsdóttir, Ó. (2003) pH dependence of the reduction of dioxygen to water by cytochrome *c* oxidase. 2. Branched electron transfer pathways linked by proton transfer. *Biochemistry 42*, 5074−5090.
(24) Georgiadis, K. E., Jhon, N.-I., and Einarsdóttir, Ó. (1994) Time-resolved optical absorption studies of intramolecular electron transfer in cytochrome *c* oxidase. *Biochemistry 33*, 9245−9256.
(25) Hill, B. C. (1994) Modeling the sequence of electron transfer reactions in the single turnover of reduced, mammalian cytochrome *c* oxidase with oxygen. *J. Biol. Chem.. 269*, 2419−2425.
(26) Oliveberg, M., Brzezinski, P., and Malmström, B. G. (1989) The effect of pH and temperature on the reaction of fully reduced and mixed-valence cytochrome *c* oxidase with dioxygen. *Biochim. Biophys. Acta 977*, 322−328.
(27) Sucheta, A., Szundi, I., and Einarsdóttir, Ó. (1998) Intermediates in the reaction of fully reduced cytochrome *c* oxidase with dioxygen. *Biochemistry 37*, 17905−17914.
(28) Bolgiano, B., Salmon, I., and Poole, R. K. (1993) Reactions of the membrane-bound cytochrome *bo* terminal oxidase of *Escherichia coli* with carbon monoxide and oxygen. *Biochim. Biophys. Acta 1141*, 95−104.
(29) Hirota, S., Mogi, T., Ogura, T., Hirano, T., Anraku, Y., and Kitagawa, T. (1994) Observation of the Fe-O_2 and Fe^{IV}=O stretching Raman bands for dioxygen reduction intermediates of cytochrome *bo* isolated from *Escherichia coli*. *FEBS. Lett. 352*, 67−70.
(30) Brittain, T., Little, R. H., Greenwood, C., and Watmough, N. J. (1996) The reaction of *Esherichia coli* cytochrome *bo* with H_2O_2: Evidence for the formation of an oxyferryl species by two distinct routes. *FEBS Lett. 399*, 21−25.
(31) Morgan, J. E., Verkhovsky, M. I., Puustinen, A., and Wikström, M. (1995) Identifiction of a "peroxy" intermediate in cytochrome bo_3 of *Esherichia coli*. *Biochemistry 34*, 15633−15637.
(32) Siletsky, S. A., Belevich, I., Jasaitis, A., Konstantinov, A. A., Wikström, M., Soulimane, T., and Verkhovsky, M. I. (2007) Time-resolved single-turnover of ba_3 oxidase from *Thermus thermophilus*. *Biochim. Biophys. Acta 1767*, 1383−1392.
(33) Smirnova, I. A., Zaslavsky, D., Fee, J. A., Gennis, R. B., and Brzezinski, P. (2008) Electron and proton transfer in the ba_3 oxidase from *Thermus thermophilus*. *J. Bioenerg. Biomembr. 40*, 281−287.
(34) Szundi, I., Funatogawa, C., Cassano, J., McDonald, W., Ray, J., Hiser, C., Ferguson-Miller, S., Gennis, R. B., and Einarsdóttir, Ó. (2012) Spectral identification of intermediates generated during the reaction of dioxygen with the wild-type and EQ(I-286) mutant of *Rhodobacter sphaeroides* cytochrome *c* oxidase. *Biochemistry 51*, 9302−9311.
(35) Han, S., Ching, Y.-C., and Rousseau, D. L. (1990) Ferryl and hydroxy intermediates in the reaction of oxygen with reduced cytochrome *c* oxidase. *Nature 348*, 89−90.
(36) Ogura, T., Takahashi, S., Shinzawa-Itoh, K., Yoshikawa, S., and Kitagawa, T. (1990) Observation of the Fe^{4+}=O stretching Raman band for cytochrome oxidase compund B at ambient temperature. *J. Biol. Chem. 265*, 14721−14723.
(37) Varotsis, C., and Babcock, G. T. (1990) Appearance of the $\upsilon(Fe^{IV}=O)$ vibration from a ferryl-oxo intermediate in the cytochrome oxidase/dioxygen reaction. *Biochemistry 29*, 7357−7362.
(38) Uchida, T., Mogi, T., and Kitagawa, T. (2000) Resonance Raman studies of oxo intermediates in the reaction of pulsed cytochrome *bo* with hydrogen peroxide. *Biochemistry 39*, 6669−6678.
(39) Ogura, T., Takahashi, S., Hirota, S., Shinzawa-Itoh, K., Yoshikawa, S., Appelman, E. H., and Kitagawa, T. (1993) Time-resolved resonance Raman elucidation of the pathway for dioxygen reduction by cytochrome *c* oxidase. *J. Am. Chem. Soc. 115*, 8527−8536.
(40) Hallén, S., and Nilsson, T. (1992) Proton transfer during the reaction between fully reduced cytochrome *c* oxidase and dioxygen: pH and deuterium isotope effects. *Biochemistry 31*, 11853−11859.

(41) Paula, S., Sucheta, A., Szundi, I., and Einarsdóttir, Ó. (1999) Proton and electron transfer during the reduction of molecular oxygen by fully reduced cytochrome *c* oxidase: A flow-flash investigation using optical multichannel detection. *Biochemistry 38*, 3025−3033.
(42) Lin, M. T., Shubin, A. A., Samoilova, R. I., Narasimhulu, K. V., Baldansuren, A., Gennis, R. B., and Dikanov, S. A. (2011) Exploring by pulsed EPR the electronic structure of ubisemiquinone bound at the Q_H site of cytochrome bo_3 from *Escherichia coli* with *in vivo* ^{13}C-labeled methyl and methoxy substituents. *J. Biol. Chem.. 286*, 10105−10114.
(43) Ingledew, W. J., Ohnishi, T., and Salerno, J. C. (1995) Studies on a stabilisation of ubisemiquinone by *Escherichia coli* quinol oxidase, cytochrome *bo*. *Eur. J. Biochem. 227*, 903−908.
(44) Sato-Watanabe, M., Itoh, S., Mogi, T., Matsuura, K., Miyoshi, H., and Anraku, Y. (1995) Stabilization of a semiquinone radical at the high-affinity quinone-binding site (Q_H) of the *Escherichia coli bo*-type ubiquinol oxidase. *FEBS Lett. 374*, 265−269.
(45) Schultz, B. E., Edmondson, D. E., and Chan, S. I. (1998) Reaction of *Escherichia coli* cytochrome bo_3 with substoichiometric ubiquinol-2: a freeze-quench electron paramagnetic resonance investigation. *Biochemistry 37*, 4160−4168.
(46) Kobayashi, K., Tagawa, S., and Mogi, T. (2000) Transient formation of ubisemiquinone radical and subsequent electron transfer process in the *Escherichia coli* cytochrome *bo*. *Biochemistry 39*, 15620−15625.
(47) Morgan, J. E., Verkhovsky, M. I., Puustinen, A., and Wikström, M. (1993) Intramolecular electron transfer in cytochrome *o* of *Escherichia coli*: Events following the photolysis of fully reduced CO-bound forms of the bo_3 and oo_3 enzymes. *Biochemistry 32*, 11413−11418.
(48) Marcus, R. A., and Sutin, N. (1985) Electron transfer in chemistry and biology. *Biochim. Biophys. Acta 811*, 265−322.
(49) Winkler, J. R., and Gray, H. B. (2014) Long-range electron tunneling. *J. Am. Chem. Soc. 136*, 2930−2939.
(50) Gray, H. B., and Winkler, J. R. (2003) Electron tunneling through proteins. *Q. Rev. Biophys. 36*, 341−372.
(51) Crane, B. R., Di Bilio, A. J., Winkler, J. R., and Gray, H. B. (2001) Electron tunneling in single crystals of *Pseudomonas aeruginosa* azurins. *J. Am. Chem. Soc. 123*, 11623−11631.
(52) Winkler, J. R., and Gray, H. B. (2014) Electron flow through metalloproteins. *Chem. Rev. 114*, 3369−3380.
(53) Morgan, J. E., Li, P. M., Jang, D.-J., El-Sayed, M. A., and Chan, S. I. (1989) Electron transfer between cytochrome *a* and copper A in cytochrome *c* oxidase: A perturbed equilibrium study. *Biochemistry 28*, 6975−6983.
(54) Ramirez, B. E., Malmström, B. G., Winkler, J. R., and Gray, H. B. (1995) The currents of life: The terminal electron-transfer complex of respiration. *Proc. Natl. Acad. Sci. U.S.A. 92*, 11949−11951.